Available online at www.sciencedirect.com
SCIENCE DIRECT®
Journal of Solid State Chemistry 178 (2005) 15–21
JOURNAL OF SOLID STATE CHEMISTRY
www.elsevier.com/locate/jssc

Crystal phase evolution of TiO_2 nanoparticles with reaction time in acidic solutions studied via freeze-drying method

Hyunho Shin[a], Hyun Suk Jung[a,*], Kug Sun Hong[a], Jung-Kun Lee[b]

[a]School of Materials Science and Engineering, Seoul National University, San 56-1, Shillim-dong, Gwanak-gu, 151-744, Seoul, Republic of Korea
[b]Los Alamos National Laboratory, Los Alamos, NM 87545, USA

Received 27 June 2004; received in revised form 10 September 2004; accepted 14 September 2004

Abstract

The crystal phase evolution of TiO_2 nanoparticles, during hydrolysis and condensation of titanium tetraisopropoxide, was quenched at various reaction times by a freeze-drying method, followed by various characterizations. Three types of solutions with different acid input times were studied: (1) addition in infinite time (no addition), (2) addition at 24 h after the hydrolysis/condensation reaction started, and (3) addition from the beginning of the reaction. The acid-free solution yielded amorphous TiO_2, which transformed to anatase very slowly. The acid input in 24 h resulted in a fast transformation of amorphous to a metastable anatase having a highly distorted atomic arrangement: thereby its transformation to a more stable phase, rutile, was suitable. The acid addition from the beginning of the reaction yielded the formation of a relatively stable anatase from the hydrolysis seed, thereby the subsequent transformation to rutile was sluggish.

Keywords: TiO_2; Crystallization; TiO_2 nanoparticle; Acid; Anatase; Rutile

1. Introduction

Recent application areas of TiO_2 in the form of the rutile phase have included optical devices such as waveguides and thin film coatings [1,2]. Anatase, another representative polymorph of TiO_2, also has been applied to many fields such as microorganism photolysis, medical treatment, photocatalyst, and electrode materials for dye-sensitized solar cells [3,4]. In order to precisely control the types of the polymorphs that are produced for appropriate applications, it is important to understand the process of crystal formation in one of the polymorphs.

Preparation methods for TiO_2 include the soft chemistry method, the hydrothermal process, and the sol–gel route [5–8]. Of these methods, the sol–gel process based on the hydrolysis and condensation of titanium alkoxide has the benefit of achieving high purity of product as compared with the sulfate or chloride processes. Furthermore, the sol–gel process is easy to apply to thin films [9,10].

It was originally believed that the only result of acid addition during hydrolysis and condensation would be the breakup of large aggregates into smaller ones through the electrostatic repulsion of charged particles [11]. However, recently, it has become known that the addition of acid has a great influence not only on the ability of the particles to gel but also on the crystal structure of TiO_2 [11,12]. In general, the process is such that the rutile phase prefers to form at a lower pH region, while the reverse is true for anatase, at a given titanium concentration [11,12]. Although the influence of the acid addition on the final crystal structure has been studied [11–14] and the growth process during post-annealing at higher temperature is available [15], the crystallization process itself during hydrolysis/condensation with the lapse of reaction time is very scarce in the literature. Furthermore, the information on the

*Corresponding author. Fax: +82 2 886 4156.
E-mail address: purey2@snu.ac.kr (H.S. Jung).

0022-4596/$ - see front matter © 2004 Elsevier Inc. All rights reserved.
doi:10.1016/j.jssc.2004.09.035

effect of acid addition time on the resultant crystal phase has not been studied. Therefore, in the present work, the crystallization process of TiO_2 has been investigated as a function of reaction time, by freeze drying the reaction product at selected reaction times. The same methodology has been applied for a series of specimens having different acid input times.

2. Experimental procedure

Titanium tetraisopropoxide (TTIP, $Ti(OiPr)_4$, 97%, Aldrich Chemical Co.) was hydrolyzed with excess water (molar ratio of water to titanium was 50) at 30 °C. The three types of investigated acid input times (t_{input}) were: (1) infinite (no addition), (2) 24 h after the hydrolysis/condensation reaction started, and (3) from the beginning of the reaction. Nitric acid was used as the source of the acid. The molar ratio of nitric acid to titanium was 0.5. This ratio value was selected via a preliminary study, in which an excess ratio formed the rutile phase so fast that it was difficult to observe the crystallization process, while a smaller amount of the acid did not yield the rutile phase. An appropriate amount of colloidal TiO_2 sol was taken from the reaction batch at different reaction intervals, followed by immediate freeze drying in liquid nitrogen for 24 h. Crystal phases were identified by X-ray diffraction (XRD, MAC Science, M18XHF-SRA). Transmission electron microscopy (TEM, JEOL JEM 200-CX) was used to investigate the morphology of the quenched reaction product. Selected area diffraction (SAD) in TEM mode and Raman spectroscopy (SPEX 1877) were used for the identification of the crystalline nature of the product.

3. Results and discussion

3.1. Overall data interpretation

Fig. 1 shows XRD patterns from each series of the specimens, i.e., $t_{input} = \infty$, $t_{input} = 24$ h, and the $t_{input} = 0$. $t_{input} = \infty$ specimen shows crystalline (anatase with a trace of brookite) peaks after about one week of total reaction time ($t_{total} = 168$ h) and the peaks grow thereafter (Fig. 1(a)). In the case of $t_{input} = 24$ h specimen (Fig. 1(b)), the peak of anatase appears with a trace of rutile relatively early: in about 12 h after the addition of acid ($t_{acid} = 12$ h, $t_{total} = 36$ h). As the reaction time lapses, the maximum peak intensity of rutile phase starts becoming higher than that of the anatase phase. The appearance of the anatase phase starts even earlier in the case of the $t_{input} = 0$ h specimen (Fig. 1(c)): the anatase phase with a trace of rutile forms appears after as early as 6 h of total reaction time ($t_{acid} = t_{total} = 6$ h) and grows thereafter. Again, the growth of the rutile phase eventually becomes more predominant than that of the anatase phase.

Fig. 2 shows bright field TEM images of samples prepared at different conditions of acid input times. The selected area diffraction (SAD) pattern of the $t_{input} = \infty$ specimen shown in inset of Fig. 2(a) shows a diffusive ring, which is indicative of the amorphous phase ($t_{total} = 24$ h). This finding confirms that the XRD patterns up to 48 h of total reaction time, shown in Fig. 1(a) result from the amorphous phase, not from the ultra-fine nature of nanocrystals. The SAD pattern shown in the inset of Fig. 2(b) ($t_{input} = 24$ h) shows spots from anatase (101) as well as rutile (110), which is in good agreement with the XRD result in Fig. 1(b) ($t_{acid} = 24$ h, $t_{total} = 48$ h). Only the anatase (101) pattern is observed in $t_{input} = 0$ specimen (Fig. 2(c)), consistent with the XRD result displayed in Fig. 1(c) ($t_{acid} = t_{total} = 24$ h specimen).

Raman spectra from each series of the specimens are shown in Fig. 3. In Fig. 3(a), the $t_{input} = \infty$ specimen ($t_{total} = 10$ min and 24 h) exhibits bands at 425 and 605 cm^{-1} simultaneously, which is interpreted to result from an amorphous or highly distorted phase in the light of Ocana et al. [16] who observed similar bands at 430 and 600 cm^{-1} at the same time. The strong anatase peak at 150 cm^{-1}, which appears in other specimens (Figs. 3(a) and (b)), is not observed. This amorphous nature of TiO_2 product up to $t_{total} = 24$ h is consistent with the XRD and TEM results found in (Figs. 1(a) and 2(a)).

In the case of the $t_{input} = 24$ h specimen (Fig. 3(b)), an evidence of crystalline phase appears as early as 10 min after the acid addition ($t_{acid} = 10$ min), as compared to the spectrum taken just before adding the acid (total = 24 h in Fig. 3(a)). Note that the crystalline phase was detected by XRD in the $t_{input} = 24$ h specimen only after the t_{acid} was about 12 h (Fig. 1(b)). However, a number of points are noteworthy for the anatase formed when $t_{input} = 24$ h. First, the peak intensity of anatase at 150 cm^{-1} decreases with time, which is contrary to the XRD result (Fig. 1(b)). This unexpected result indicates that the global atomic arrangement of anatase, detected by XRD, increases with time, whereas local atomic arrangement of anatase, based on Raman, becomes more distorted. Second, in the spectrum from 10 min specimen in Fig. 3(b), the Raman peaks are shifted from the positions of anantase (A: 515 cm^{-1}) and rutile (R: 605 cm^{-1}). Furthermore, a broadband at 400–440 cm^{-1} was noticed. These results indicate that this specimen has a highly distorted local atomic arrangement (we denote the anatase with a highly distorted crystalline structure as AN* in this work for later purpose). Thus, the absence of specific peaks in the XRD results of $t_{acid} = 10$ min and 6 h samples (Fig. 1(b)) results from a highly distorted crystal structure as opposed to an amorphous nature.

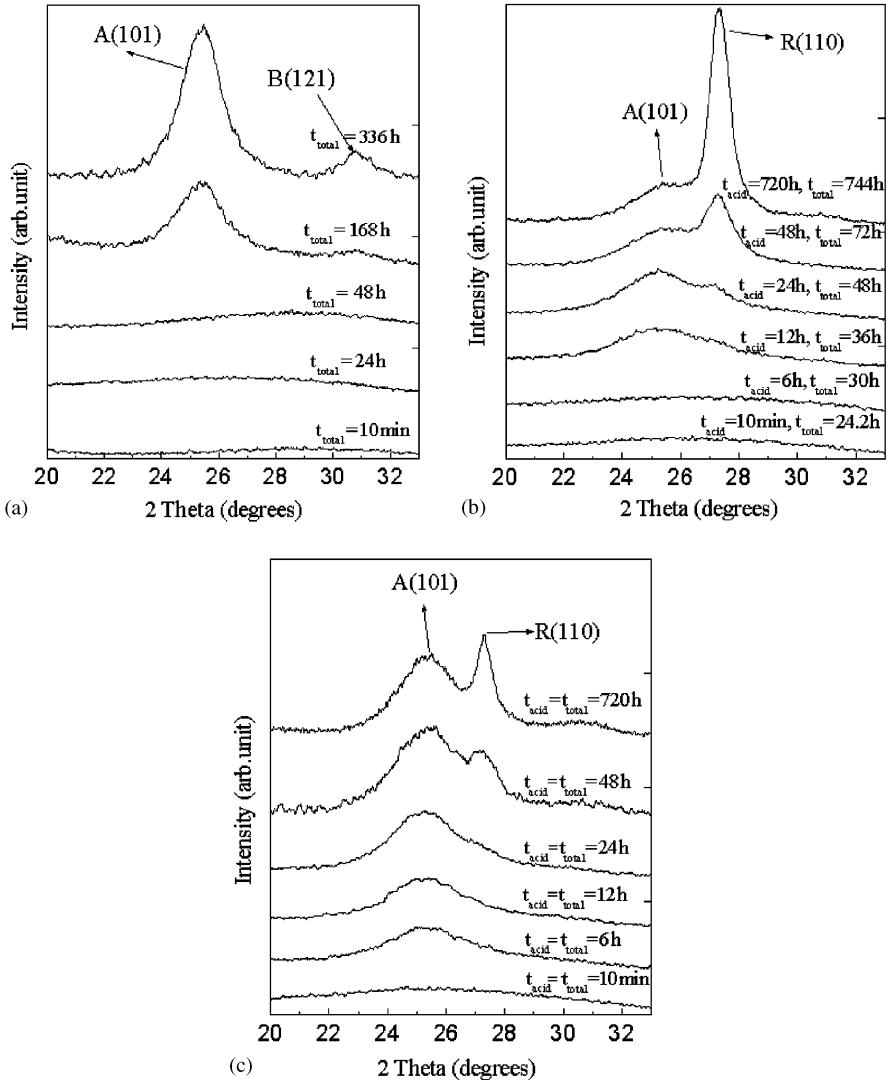

Fig. 1. XRD patterns from: (a) $t_{input} = \infty$, (b) $t_{input} = 24$ h, and (c) $t_{input} = 0$ specimens. A: anatase, B: Brookite, and R: rutile.

For the $t_{input} = 0$ specimen (Fig. 3(c)), although the crystalline phase appears when t_{acid} was about 6 h in XRD (Fig. 1(c)), there is evidence of the anatase crystalline phase as early as when the t_{acid} had been 10 min in the Raman spectrum. Since no apparent peaks are observed either at about 605 or 425 cm^{-1} in this specimen, the presence of amorphous TiO_2 would not be significant. This finding indicates that the lack of appreciable XRD peaks in the 10 min sample displayed in Fig. 1(c) result from the ultrafine nature of the nanocrystals, not from the amorphous phase. The peak intensity of anatase at 150 cm^{-1} in Fig. 3(c) increases with time, which is consistent with the XRD result (Fig. 1(c)). This result indicates that the local atomic arrangement of anatase in this case is relatively well maintained, compared to the specimen when $t_{input} = 24$ h (Fig. 3(b)), in which the local crystallinity was not maintained in a global scale (AN*).

3.2. TiO_2 crystallization under no acid ($t_{input}=\infty$)

In order to investigate the evolution of anatase and rutile phases with reaction time, maximum XRD peak intensities in Fig. 1 are plotted as a function of total reaction time in Fig. 4. As seen in Fig. 4, under the absence of acid ($t_{input} = \infty$), the crystallization process of anatase from the amorphous phase is extremely slow until after about a week ($t_{total} = 168$ h). Bischoff and Anderson [11] also reported similar results when the newly forming TiO_2 from the hydrolysis of titanium ethoxide at room temperature was amorphous in XRD and crystallized to anatase with a trace of brookite after about 3–5 weeks of aging. Bischoff and Anderson suggested that the initial hydrolysis product could be crystalline, because it was unclear why such a slow aging caused the formation of a mixture of metastable polymorphs. Thus, Bischoff and Anderson interpreted

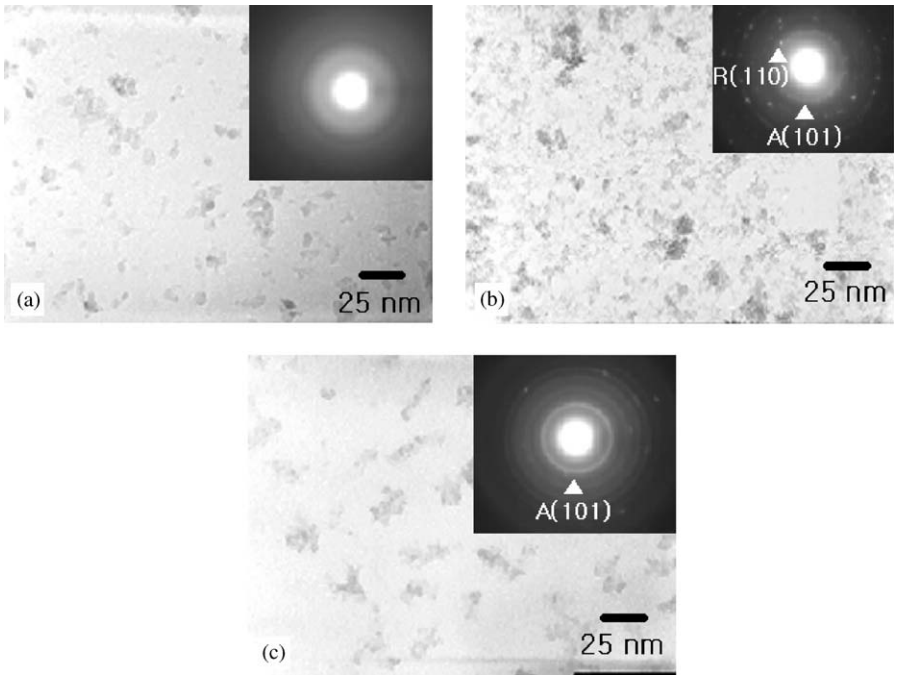

Fig. 2. Bright field TEM images of: (a) $t_{input} = \infty$, (b) $t_{input} = 24$ h, and (c) $t_{input} = 0$ specimens. Total reaction times were 24, 48 ($t_{acid} = 24$ h), and 24 h ($t_{acid} = 24$ h), respectively.

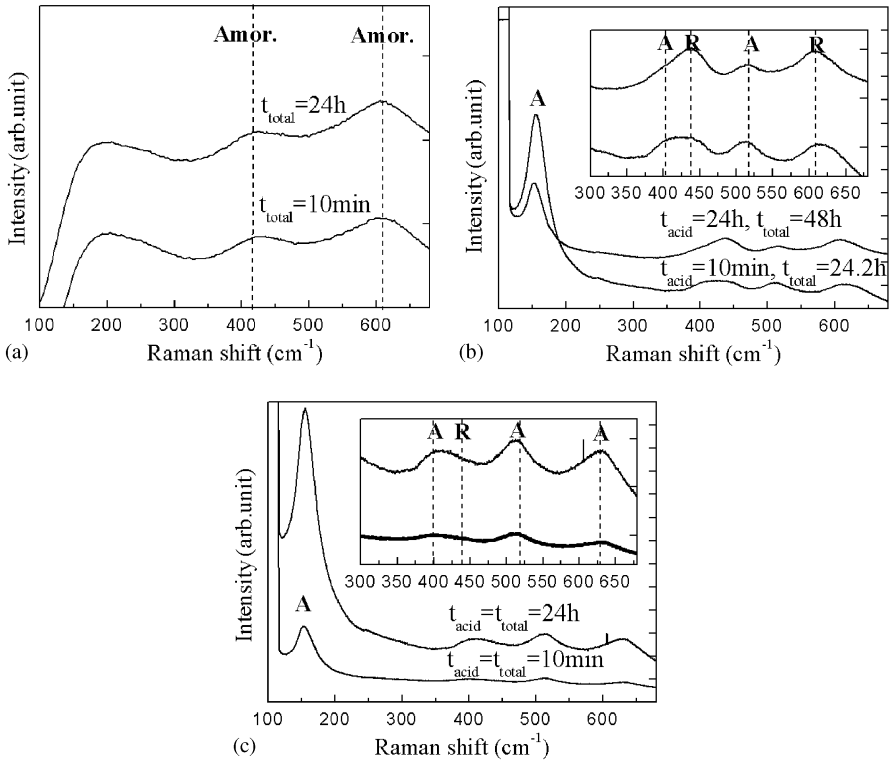

Fig. 3. Raman spectra from: (a) $t_{input} = \infty$, (b) $t_{input} = 24$ h, and (c) $t_{input} = 0$ specimens.

from their XRD results that the crystallites were too small to be detected by XRD as crystalline. However, from the additional evidence of the SAD (Fig. 2(a)) and Raman spectrum (Fig. 3(a)) in this work, which show the apparent formation of amorphous phase in the initial product, the anatase with a trace of brookite in

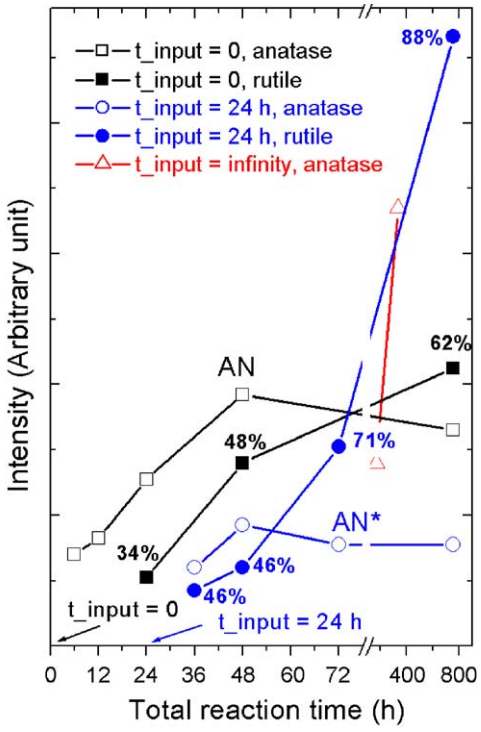

Fig. 4. Change in maximum XRD peak intensities in Fig. 1 as a function of total reaction time. Percentages shown near the rutile phase markers indicate the relative rutile/antase phase ratio calculated by XRD intensity ratio by the method shown elsewhere.

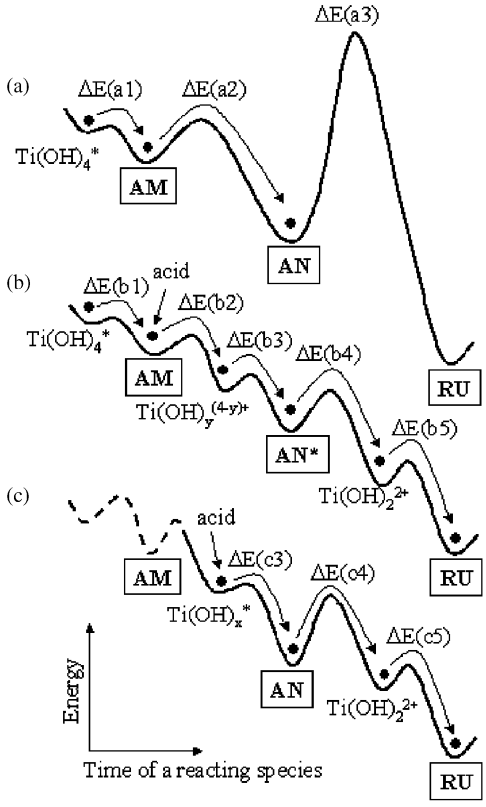

Fig. 5. Activation energy diagram for the crystallization process when: (a) $t_{input} = \infty$, (b) $t_{input} = 24$ h, and (c) $t_{input} = 0$. AM: amorphous TiO_2, AN: anatase, AN*: anatase with a highly distorted local atomic arrangement, and RU: rutile.

both Bischoff and Anderson's and our work is shown not to directly form from the hydrolysis, but to crystallize from the amorphous TiO_2 phase.

The activation energy diagram for the TiO_2 crystallization process in acid-free solution ($t_{acid} = \infty$) is shown in Fig. 5(a). In a non-acidic titanium solution, the dissolved titanium species in equilibrium with TiO_2 is $Ti(OH)_4$ [14]. Titanium tetraisopropoxide reacts very quickly with water, especially in the presence of a very large stoichiometric excess of water. The very rapid initial hydrolysis results in a solution with a high degree of supersaturation of hydroxylated titanium, i.e., it yields an activated complex, $Ti(OH)_4$*. This result may lead to a high rate of nucleation of the most unstable condensed form of the TiO_2, i.e., the amorphous phase (denoted as AM in Fig. 5(a)). The rapid formation of the amorphous phase (Fig. 3(a)) implies that the activation energy for $Ti(OH)_4^* \rightarrow AM$, $\Delta E(a1)$, is fairly low. Transformation of this amorphous phase to anatase is interpreted to require a higher activation energy than the previous process, i.e., $\Delta E(a2) > \Delta E(a1)$ as it takes quite a long period of time in an acid-free environment. Once anatase forms, its transformation to rutile does not seem to be possible in the non-acidic solution at 30 °C because it requires too high an activation of energy ($\Delta E(a3)$): in general, the anatase to rutile transformation requires a temperature range between 400 and 1200 °C in a solid-state reaction [17,18].

3.3. TiO_2 crystallization when acid is added in 24 h of reaction time (t_{input}=24 h)

In the $t_{input} = 24$ h specimen, the crystallization of TiO_2 ($t_{total} = 24.2$ h in Fig. 3(b)) took place in the previously formed amorphous TiO_2 before adding the acid ($t_{total} = 24$ h in Fig. 3(a)). As seen in Fig. 4, a detectable amount of anatase by XRD appeared about 12 h after the input of acid ($t_{acid} = 12$ h, $t_{total} = 36$ h): this appearance is fairly early as compared to the acid-free specimen which required about a week. This finding indicates that the activation energy of the transformation from the amorphous to the anatase phase has been significantly lowered in the acidic solution (Fig. 5(b)) as compared to the non-acidic solution (Fig. 5(a)). A plausible reason for the lowering of the activation energy in the acidic solution is that the solubility of TiO_2 into $Ti(OH)_4^{(4-y)+}$ increases with the acid addition [11,19]. Thus, a new two-step reaction path, i.e., a dissolution/reprecipitation process would lower the activation energy i.e., $\Delta E(b2) < \Delta E(a2)$ and $\Delta E(b3) < \Delta E(a2)$, so that the crystallization of the amorphous phase into the anatase phase was facilitated in the acidic solution. We denote anatase as AN* in Fig. 5(b) instead of AN because, as previously mentioned, anatase

forming in an acidic solution ($t_{input} = 24$ h) has a highly distorted crystalline structure (Fig. 3(b)). Furthermore, the XRD peak intensities (Fig. 4) of anatase in this case ($t_{input} = 24$ h) are significantly lowered as compared with the case of the acid-free solution ($t_{input} = \infty$). Thus, the anatase (AN*) forming rapidly in an acidic solution ($t_{input} = 24$ h) is thermodynamically less stable than that (AN) forming in an acid-free solution ($t_{input} = \infty$).

The most remarkable phenomenon in the $t_{input} = 24$ h specimen in Fig. 4 is that, after the anatase and rutile phase grow until reaching $t_{acid} = 24$ h ($t_{total} = 48$ h), the rutile phase predominantly grows thereafter by consuming anatase. This discovery indicates that anatase transforms to the thermodynamically most stable form, rutile, even at 30 °C in the acidic solution. Thus, the activation energy of the transformation of anatase to rutile is significantly lowered in this acidic solution as compared with the solid-state reaction [17,18]. It was previously pointed out that anatase could not change to rutile under low-temperature hydrothermal conditions in HCl solutions [15], presumably due to a lack of sufficient activation energy at a low temperature. However, our result clearly indicates a transformation of anatase to rutile even at 30 °C in the acidic solution. Although the temperature was not as low as the one in the current work, Wu et al. [20] and Oskam et al. [15] also recently reported that a treatment of an encapsulated sol product at 200–220 °C yielded transformation of anatase to rutile. Therefore, it is necessary to consider the reason why such anatase to rutile conversion can be achieved at such low temperatures in solution.

The apparent pH of the solutions by acid additions in the current work was 0.66 and the initial concentration of Ti during hydrolysis/condensation step was about 0.02. In this highly acidic and titanium-dilute condition, the most predominant Ti(IV) ionic species is $Ti(OH)_2^{2+}$ [19]. In the theoretical prediction by Lencka and Riman, based on the ideal solution approximation [19], there is a solution condition ([Ti^{4+}] and pH) where the order of the magnitude of the chemical potentials is $u_{ru} < u_i < u_{an}$, where u is the chemical potential and subscripts ru, i, and an are rutile, $Ti(OH)_2^{2+}$, and anatase, respectively. In the experimental observation by Yamabi and Imai [19], our solution condition is the case where the order of chemical potential is $u_{ru} < u_i < u_{an}$. Thus, it is hypothesized that the new reaction path from anatase via $Ti(OH)_2^{2+}$ to rutile is the low-activation-energy path: $\Delta E(b4) < \Delta E(a3)$ and $\Delta E(b5) < \Delta E(a3)$ (Fig. 5) in the acidic solution ($t_{input} = 24$ h). If the new two-step reaction path lowers the activation energy as such, the transformation of anatase to rutile would be achieved at a fairly reduced temperature. Recapitulating, the new low-activation-energy path involves the dissolution of anatase to the metastable phase $Ti(OH)_2^{2+}$, followed by the reprecipitation to the stable rutile phase.

3.4. TiO_2 crystallization when acid is added initially (t_{input}=0)

In a case where acid is added from the beginning of the hydrolysis reaction, the anatase phase forms at the early stage of the reaction from the seed of the hydrolysis product (Fig. 3(c)). Since the crystalline phases almost simultaneously form at a fairly early reaction time, the acid is believed to foster the hydrolysis itself as well.

The appreciable XRD peak intensity from anatase appears as early as $t_{acid} = t_{total} = 6$ h (Fig. 1(c) and Fig. 4), where the growth rate is even faster than the case when $t_{input} = 24$ h. For the interpretation of this phenomenon, it is informative to refer to the activation energy diagram shown in Fig. 5(c). As previously mentioned, the initial hydrolysis reaction in the affluent water condition is fast so that an activated complex $Ti(OH)_4$* forms. The addition of the acid from the beginning of the hydrolysis reaction is interpreted to form a new activated complex $Ti(OH)_x$*, whose chemical potential is located between amorphous (AM) and anatase (AN) (Fig. 5(c)) because, as previously noted, there is no apparent involvement of the amorphous phase at the initial stage of anatase formation. The activation energy of the transformation from $Ti(OH)_x$* to anatase ($\Delta E(c3)$) must be fairly low considering that the process is fairly rapid.

As the addition of acid from the beginning of hydrolysis reaction greatly facilitates the formation of anatase, its XRD peak intensity of anatase in Fig. 4 is higher than the anatase formed when $t_{input} = 24$ h. This observation indicates that acid addition from the beginning of the reaction favors the thermodynamically more stable anatase (AN) as compared to the anatase formed when $t_{input} = 24$ h (AN* in Fig. 5(b)).

In-depth comparisons of the XRD results in Fig. 4 for $t_{input} = 0$ and $t_{input} = 24$ h specimens yield some more important features indicating that the former shows a more sluggish formation of rutile. First, the growth of the rutile phase when $t_{input} = 0$ is slower than the case of $t_{input} = 24$ h: a detectable amount of rutile by XRD appears when t_{acid} is 24 h ($t_{total} = 24$ h) in the $t_{input} = 0$ specimen, while a detectable amount of rutile by XRD only appears when t_{acid} is 12 h ($t_{total} = 36$ h) in the case of the $t_{input} = 24$ h specimen. Second, the peak intensity of rutile overtakes that of anatase later in the $t_{input} = 0$ specimen than in the $t_{input} = 24$ h specimen. Third, the XRD peak intensity of the fully grown rutile at $t_{total} = 720$ h is much lower in the $t_{input} = 0$ h specimen than in the $t_{input} = 24$ h specimen. These observations, i.e., a more sluggish formation of rutile from anatase for the case of the acid addition from the beginning, result from the thermodynamically more stable nature of anatase when $t_{input} = 0$ (AN) as compared to the case when $t_{input} = 24$ h (AN*: a highly distorted crystalline

arrangement). This finding is illustrated using the activation energy diagram shown in Fig. 5(c). As seen in Fig. 5(c), the dissolution of AN ($t_{input} = 0$) to form $Ti(OH)_2^{2+}$ in the acidic solution is more difficult as compared to the case of AN* ($t_{input} = 24$ h) since the energy well of AN is deeper than AN*. Therefore, $\Delta E(c4)$ is higher than $\Delta E(b4)$, yielding a sluggish transformation of anatase to rutile.

4. Conclusion

The effect of acid addition time on the crystal phase evolution of TiO_2 nanoparticles, during hydrolysis and condensation of titanium tetraisopropoxide at 30 °C, was investigated by quenching the samples at selected reaction times, followed by characterizations using X-ray diffraction, transmission electron microscopy, and Raman spectroscopy. When no acid was added during the reaction, which corresponded to the addition in infinite reaction time, the amorphous TiO_2 phase formed first from a supersaturated titanium hydroxylate, followed by a very slow crystallization to a thermodynamically metastable phase, anatase. The subsequent conversion from anatase to rutile was not observed.

For the case when nitric acid was added in total reaction time of 24 h, crystallization of anatase from the previously formed amorphous phase was greatly facilitated as compared to the acid-free solution. The rapid amorphous to anatase transformation resulted in a highly distorted crystalline structure of the anatase as compared to the acid-free counterpart. The subsequent conversion of anatase to the thermodynamically more stable phase, rutile, was achieved via a low-activation-energy path: it was interpreted to involve the dissolution of anatase to $Ti(OH)_2^{2+}$ and its reprecipitation into rutile.

When the acid was added from the beginning of the hydrolysis reaction, the anatase phase formed directly from the seed of the hydrolysis product with negligible involvement of the amorphous phase. In such a case, the crystallinity of the anatase phase was higher than the case when $t_{input} = 24$ h, and thus its activation energy of dissolution was higher, resulting in a sluggish conversion of anatase to rutile.

Acknowledgment

This work was supported by the Ministry of Commerce, Industry and Energy, Korea. The authors are also grateful to the Research Institute for Advanced Materials at Seoul National University.

References

[1] J.-Y. Gan, Y.C. Chang, T.B. Wu, Appl. Phys. Lett. 72 (1998) 332.
[2] A. Fujishima, T.N. Rao, D.A. Tryk, Photochem. Photobiol. C 1 (2000) 1.
[3] R. Cai, Y. Kubota, T. Shuin, K. Hashimoto, A. Fujishima, Cancer Res. 52 (1992) 2346.
[4] M.R. Hoffmann, S.T. Martin, W. Choi, D.W. Bahnemann, Chem. Rev. 95 (1995) 69.
[5] R.A. Spurr, H. Myers, Anal. Chem. 29 (1957) 760.
[6] P.S. Ha, H.J. Youn, H.S. Jung, K.S. Hong, Y.H. Park, K.H. Ko, J. Colloid Interf. Sci. 223 (2000) 16.
[7] K.N.P. Kumar, Scr. Mater. 32 (1995) 873.
[8] M. Ocana, J.V.G. Ramos, C.J. Serna, J. Am. Ceram. Soc. 75 (1992) 2010.
[9] H. Yin, Y. Wada, T. Kitamura, T. Sumida, Y. Hasegawa, S. Yanagida, J. Mater. Chem. 12 (2002) 378.
[10] S.D. Park, Y.H. Cho, W.W. Kim, S.J. Kim, J. Solid State Chem. 146 (1999) 230.
[11] B.L. Bischoff, M.A. Anderson, Chem. Mater. 7 (1999) 1772.
[12] S. Yamabi, H. Imai, Chem. Mater. 14 (2002) 609.
[13] J. Yang, S. Mei, J.M.F. Ferreira, J. Am. Ceram. Soc. 83 (2000) 1361.
[14] F. Cot, A. Larbot, G. Nabias, L. Cot, J Eur. Ceram. Soc. 18 (1998) 2175.
[15] G. Oskam, A. Nellore, R.L. Penn, P.C. Searson, J. Phys. Chem. B 107 (2003) 1734.
[16] M. Ocana, J.V.G. Ramos, C.J. Serna, J. Am. Ceram. Soc. 75 (1992) 2010.
[17] F.C. Gennari, D.M. Pasquevich, J. Mater. Sci. 33 (1998) 1571.
[18] R.L. Penn, J.F. Banfield, Am. Mineral. 84 (1999) 871.
[19] M.M. Lencka, R.E. Riman, Chem. Mater. 5 (1993) 61.
[20] M. Wu, G. Lin, D. Chen, G. Wang, D. He, S. Feng, R. Xu, Chem. Mater. 14 (2002) 1974.